Macromolecules

Article

pubs.acs.org/Macromolecules

One-Pot Synthesis of Elastomeric Monoliths Filled with Individually Encapsulated Liquid Droplets

Inna Gurevitch and Michael S. Silverstein*

Department of Materials Engineering, Technion - Israel Institute of Technology, Haifa 32000, Israel

Supporting Information

ABSTRACT: The ability to encapsulate and store liquids within discrete, micrometer-scale containers is essential for living organisms and is used by water-storage cells to keep plants healthy, even during a prolonged drought. This paper describes the one-pot synthesis of liquid droplet elastomers (LDEs), a novel materials system with advantageous properties. LDEs are tissue-like elastomeric monoliths that contain around 85% water in the form of individually encapsulated micrometer-scale droplets. The LDE structure is templated within high internal phase Pickering emulsions, emulsions stabilized by nanoparticles that also function as cross-linking centers. The polyhedral shapes of the droplets, which accommodate the high volume fraction of water, are "locked-in" to the LDE during polymerization. The water retention in these unique materials is exceedingly high, and as seen for living systems, the presence of the encapsulated water droplets enhances the resistance to compressive deformation and to ignition upon direct exposure to a flame.

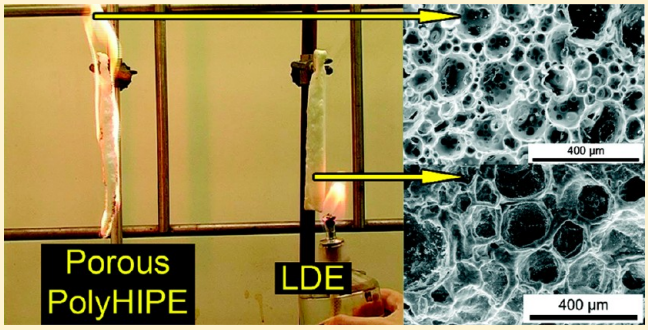

INTRODUCTION

The ability to encapsulate and store liquids within discrete, micrometer-scale containers is essential for living organisms. Water-storage cells can keep plants healthy even during a prolonged drought.[1] There are many examples of encapsulated water within living systems. Vacuoles are specialized water storage systems found in all plant and fungal cells as well as in some protist, animal, and bacterial cells.[2] The vacuole wall, a vesicle membrane, forms an enclosed compartment containing inorganic and organic molecules in an aqueous solution. The cortex of cacti and the leaves of many succulents contain specialized cells with flexible, elastic walls. The presence of encapsulated water significantly influences the system's behavior and its mechanical properties.[3] The encapsulation of liquids in such discrete, micrometer-scale containers is also essential in both the pharmaceutical and cosmetic industries.[4] Developing methods whereby discrete water droplets could be encapsulated within monolithic synthetic polymers could yield novel materials systems with advantageous properties.

Emulsion-templated porous polymers have been synthesized within high internal phase emulsions (HIPEs), usually defined as emulsions containing over 74% individual droplets of the internal phase, although HIPEs can often contain as much as 90% internal phase.[5,6] The polymerization of monomers within a HIPE's continuous, external phase is used to synthesize emulsion-templated, monolithic, porous polymer systems termed polyHIPEs.[7−10] Water-in-oil, oil-in-water, oil-in-oil, and CO_2-in-water HIPEs have all been used to synthesize polyHIPEs.[10−13] The mechanical stability of polyHIPEs is almost always enhanced through the addition of cross-linking comonomers to the external phase.

Significant amounts of amphiphilic surfactants, sometimes 20−30% of the external phase, are usually used to prevent phase separation in HIPEs. Surfactant-stabilized HIPEs tend to have droplet sizes on the order of tens of micrometers. Micrometer-sized holes are formed in the polymer walls during synthesis and/or processing, yielding a continuous internal phase which can be easily removed. The resulting porous polymer has a highly interconnected open-cell porosity that reflects the internal phase content and a porous structure that reflects the sizes of the droplets and the holes. A wide variety of polyHIPE-based polymeric systems have been synthesized including copolymers,[14−16] interpenetrating polymer networks (IPN),[17] crystallizable side chain polymers,[18,19] biocompatible polymers,[20−27] functional surfaces,[28−30] bicontinuous polymers,[31−33] and organic−inorganic hybrids and composites.[34−43]

Pickering emulsions are surfactant-free emulsions stabilized by amphiphilic solid particles that preferentially migrate to the oil−water interface and prevent droplet coalescence.[44] Recently, porous polyHIPEs have been synthesized using particle-stabilized high internal phase Pickering emulsions as templates.[33,45−50] The resulting polyHIPEs tend to have structures on the order of hundreds of micrometers that seem to be less interconnected and more closed-cell-like. There is, however, a certain degree of interconnectivity in these

Received: May 18, 2012
Revised: July 6, 2012
Published: August 10, 2012

 © 2012 American Chemical Society

materials since the internal phase can usually be removed with ease. Silane-modified silica nanoparticles (NPs) proved especially effective for stabilizing HIPEs for polyHIPE synthesis.[51,52] The porous structure was shown to be strongly affected by the internal phase content, the type and amount of particles used for stabilization, and the locus of initiation. Individual droplets were shown to remain intact and compartmentalized in water-in-oil HIPEs containing polymer particles that swell to form a HIPE gel.[53]

This paper describes the one-pot synthesis of liquid droplet elastomers (LDEs), tissue-like monoliths consisting of individual water droplets, each encapsulated within a thin, elastomeric membrane. The LDE structure is templated within high internal phase Pickering emulsions, emulsions stabilized using nanoparticles that also function as cross-linking centers. Four different HIPE-templated materials will be described: (1) PH-1, a typical comonomer-cross-linked polyHIPE, from a surfactant-stabilized HIPE; (2) LDE-1 from a nanoparticle-stabilized HIPE polymerized using a water-soluble free-radical initiator; (3) PH-2 from a nanoparticle-stabilized HIPE polymerized using an organic-soluble free-radical initiator; (4) LDE-2 from a nanoparticle-stabilized HIPE polymerized using nanoparticle-initiated atom transfer radical polymerization (ATRP). The recipes for these four HIPEs are listed in Table 1. Varying the type of liquid encapsulated and/or the type of polymer could be used to enhance the LDE's functionality for particular applications. For example, entrapped water could be used for self-extinguishing fire retardation, entrapped disinfectant could be used for a disinfecting seal, or entrapped dye could be used to indicate the site of puncture. These synthesis guidelines can be used with other acrylate monomers to generate novel polymer systems with properties of interest.[54]

Table 1. HIPE Recipes

		content, wt %			
phase	component	PH-1	PH-2	LDE-1	LDE-2
external, organic phase	EHA	11.46	14.08	14.06	14.80
	M-NPs	0	0.75	0.74	0
	MC-NPs	0	0	0	0.96
	$CuBr_2$	0	0	0	0.06
	bpy	0	0	0	0.04
	water	0	0	0	0.96
	SMO	4.05	0	0	0
	DVB	2.96	0	0	0
	BPO	0	0.17	0	0
	total	18.47	15.00	14.80	16.82
internal, aqueous phase	water	80.97	84.58	84.43	83.12
	KPS	0.16	0	0.35	0
	K_2SO_4	0.40	0.42	0.42	0
	AA	0	0	0	0.06
	total	81.53	85.00	85.20	83.18

EXPERIMENTAL SECTION

Materials. The monomer used for all the HIPEs, 2-ethylhexyl acrylate (EHA, Aldrich), was washed to remove the inhibitor (three times with a 5 wt % sodium hydroxide solution and then three times with deionized water). A stabilizing salt, potassium sulfate (K_2SO_4, Frutarom, Israel), was added to the aqueous phase when conventional free-radical initiation was used (PH-1, PH-2, and LDE-1). The comonomer used to cross-link PH-1, the typical polyHIPE used as a reference material, was divinylbenzene (DVB, containing 20% ethylstyrene, Aldrich). DVB was washed as described above for EHA. The DVB was needed in the surfactant-stabilized polyHIPE since un-cross-linked PEHA is viscous and tacky, and the polyHIPE would have collapsed during drying. Using DVB as a cross-linking comonomer has been shown to enhance chain stiffness and yield an increase in modulus.[37] The surfactant used to stabilize this typical polyHIPE was sorbitan monooleate (SMO, Span 80, Fluka Chemie).

The Pickering HIPEs (PH-2, LDE-1, and LDE-2) were stabilized using alkoxysilane functionalized fumed silica nanoparticles (NPs) with an average diameter of 7 nm and a surface area of 390 m^2/g (Sigma). The NPs for the polymers synthesized using conventional free-radical polymerization (PH-2 and LDE-1) were termed M-NPs. M-NPs were functionalized to produce double bonds on their surfaces using 3-(methacryloxy)propyltrimethoxysilane (MPtMS, 248.3 g/mol, Alfa Aesar).[52] The methoxysilane groups undergo hydrolysis and condensation, bond to the silica surface, and form a three-dimensional network of groups containing double bonds that can copolymerize with EHA. The initiator-bearing NPs for the polymers synthesized using ATRP were termed MC-NPs. MC-NPs had three functions, stabilizing the HIPE, initiating the polymerization, and acting as cross-linking centers. MC-NPs were functionalized to produce both double bonds for copolymerization with EHA and groups for ATRP initiation using a combination of MPtMS and *p*-chloromethylphenyltrimethoxysilane (CMPtMS, 246.8 g/mol, Gelest). Surface modification of the NPs took place in a solution of ethanol (Bio Lab), acetic acid (Merck), and deionized water.

Three different initiator systems were used: conventional free-radical initiators (water-soluble and organic-soluble) and activators generated by electron transfer (AGET) for NP-initiated ATRP.[51,55−57] The water-soluble free-radical initiator was potassium persulfate (KPS, $K_2S_2O_8$, Riedel-de-Haen). The organic-soluble free-radical initiator was benzoyl peroxide (BPO, Fluka Chemie). The AGET ATRP initiator system consisted of a catalyst ($CuBr_2$, Sigma-Aldrich), a ligand (2,2-bipyridine, bpy, Sigma-Aldrich), a reducing agent (ascorbic acid, AA, Sigma-Aldrich), and an initiator (the CMPtMS on the MC-NPs).

Nanoparticle Modification. An ethanol/water solution (95 vol % ethanol) and an aqueous acetic acid solution (5.5 vol % acetic acid, 1 M) were prepared. The pH of the ethanol solution was adjusted to 4.5 by adding 3 vol % of the acetic acid solution. To produce M-NPs, MPtMS, at 4.2 wt % of the solvents, was added and left for 1 h. Silica NPs, at 0.7 wt % of the solvents, were then added. The mass ratio of MPtMS to silica was 6. To produce MC-NPs, MPtMS and CMPtMS, at 5.0 wt % of the solvents each, were added and left for 1 h. Silica NPs, at 1.4 wt % of the solvents, were then added. The mass ratios of MPtMS and CMPtMS to silica were each 3.6.[52] The silane−silica mixture was stirred for 1 h. The NPs were then filtered using Whatman No. 1 filter paper and dried overnight at 70 °C in a convection oven.

Polymer Synthesis. The aqueous and organic phases were prepared separately (Table 1). The aqueous phase was slowly dripped into the organic phase with continuous stirring.[52] The resulting HIPEs were covered with aluminum foil and polymerized in a circulating air oven at 65 °C for 24 h without stirring. The PH-1 and PH-2 were dried in a freeze-dryer (Christ, Alpha 1-2 LD plus) for ∼48 h.

The HIPE formation was slightly more complex for LDE-2. The aqueous phase consisted of an AA solution. $CuBr_2$ and bpy were dissolved in a small amount of water and then added to the organic phase to minimize their exposure to AA until the HIPE was fully formed. The organic phase was cooled in an ice bath and remained in the ice bath as the aqueous phase was dripped in slowly with constant stirring. The stirring was stopped after the entire aqueous phase was added, and a second AA solution, identical to that added to the aqueous phase, was poured over the HIPE. This second AA solution remained above the highly viscous HIPE during polymerization and minimized the direct contact of the HIPE with air.[51] The HIPE was covered with aluminum foil and polymerized in a circulating air oven at 80 °C for 24 h without stirring. The second AA solution was removed following polymerization.

Characterization. The porous structure was characterized using low-vacuum SEM of uncoated cryogenic fracture surfaces (FEI Quanta 200, 20 kV). The average polyHIPE void sizes were calculated from

dx.doi.org/10.1021/ma301007s | Macromolecules 2012, 45, 6450−6456

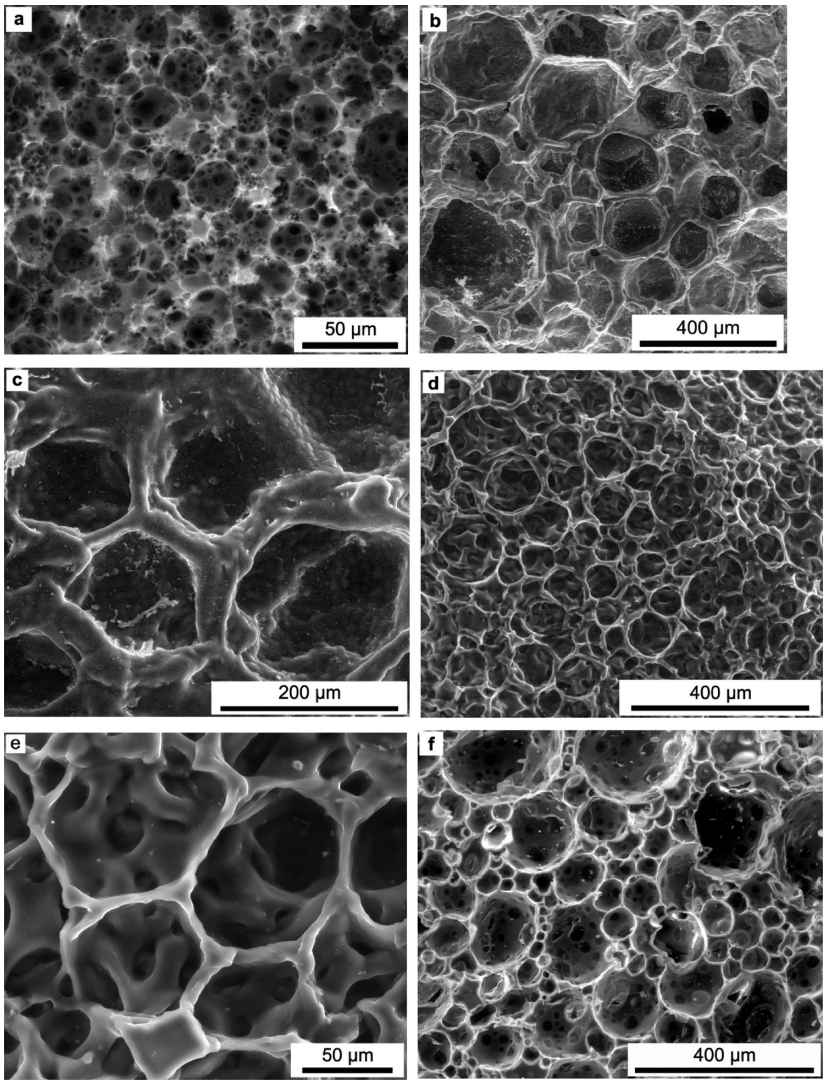

Figure 1. SEM micrographs of monolith cross sections from cryogenic fracture: (a) PH-1, (b, c) LDE-1, (d, e) LDE-2, and (f) PH-2.

the SEM micrographs using a correction for the statistical nature of the cross section.[58] The wall structure was characterized using TEM. TEM specimens 70−80 nm thick for transmission electron microscopy (TEM, FEI Technai G^2 T20 S-Twin, operating at 200 kV) were prepared using ultramicrotomy (Ultracut E, Reichert-Jung). Ultramicrotomy specimens from the porous PH-2 were prepared through vacuum infiltration (for about 1 h) with methyl methacrylate (MMA, Aldrich) containing 1 wt % BPO. The MMA was then polymerized in a circulating air oven at 50 °C. TEM specimens from the water-filled LDEs were prepared using cryo-ultramicrotomy. The water in the LDE specimens was removed by allowing them to dry at room temperature.

Water retention was measured for cylindrical specimens, 4.7 cm in diameter and 1.5 cm in height (total volume, 26 cm^3). The specimens were placed in the back of an operational chemical hood in open Petri dishes such that 70% of the surface area was exposed to ambient atmosphere at room temperature. The specimens were weighed initially to determine the initial specimen mass, $M(0)$. The specimen mass, $M(t)$, was measured at various intervals of time. For PH-2, the mass of the polymer in the specimen, $M(\infty)$, was measured after all the water was removed. For LDE-1 and LDE-2, from which it was difficult to remove all the water, $M(\infty)$ was estimated from the feed composition. The mechanical behavior was evaluated through uniaxial compressive stress−strain tests. Compressive stress−strain measurements were carried out on 5 × 5 × 5 mm^3 cubes at 10%/min until displacement limitations were reached (Lloyd Tensile Machine). The materials were tested undried.

RESULTS AND DISCUSSION

Structure. The structure of the cryogenic fracture surface of PH-1, seen in Figure 1a, is typical of surfactant-stabilized polyHIPEs. This structure, consisting of relatively thin polymer walls surrounding relatively small, polydisperse, highly interconnected, spherical voids, results from the ability of surfactants to stabilize relatively small droplets, the partial droplet coalescence and Ostwald ripening as the polymerization proceeds, and the formation of ruptures at the thinnest point in the polymerizing monomer envelope surrounding the water droplets. The structure of the cryogenic fracture surface of the NP-stabilized LDE-1, seen in Figure 1b,c, is quite different. The polyhedral nature of the structure reflects the shapes adopted by the droplets that allows the HIPEs to attain such high internal phase volume fractions. Interfacial initiation, synthesis that begins at the oil−water interface, "locks in" the polyhedral droplet shapes and prevents droplet coalescence, Ostwald ripening, and the formation of a more polydisperse spherical structure.[51,52] The polyhedra in Figure 1b,c have a bimodal size distribution with averages of 70 and 410 μm. The structure of

dx.doi.org/10.1021/ma301007s | *Macromolecules* 2012, 45, 6450−6456

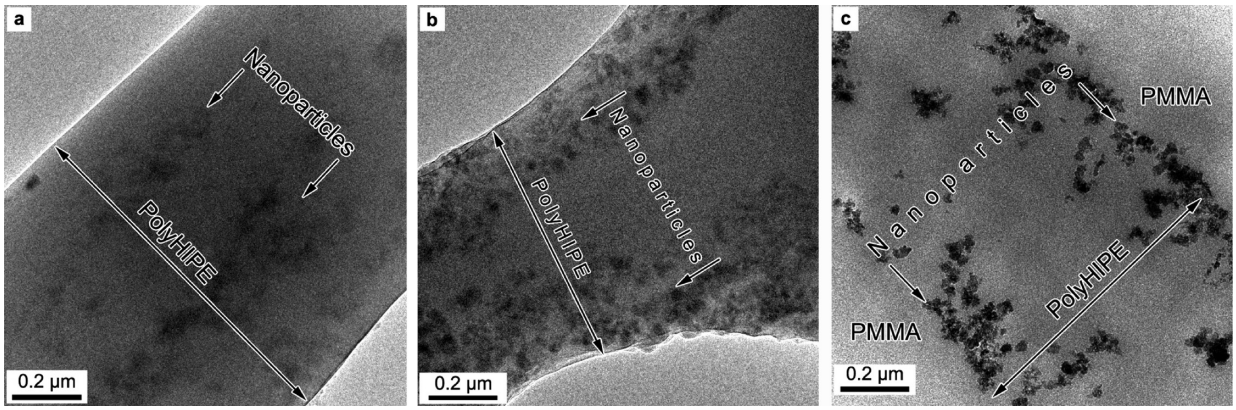

Figure 2. TEM micrographs of wall cross sections from ultramicrotomy: (a) LDE-1, (b) LDE-2, and (c) PH-2.

NP-stabilized LDE-2 in Figure 1d,e is similar to that of LDE-1 in Figure 1b,c. However, the structure in LDE-2, a bimodal size distribution with averages of 60 and 115 μm, is significantly smaller than that of LDE-1.

Previous work has shown that the nanoparticles in polymerized Pickering HIPEs exhibit several different types of behavior, depending upon the nature of the nanoparticle surface and the locus of initiation: (1) when initiation takes place at the oil–water interface, then diffusion of the monomer forces the nanoparticles into the wall, as illustrated schematically in Figure 3a,c; (2) when initiation takes place within the organic phase or at NP surfaces, then the nanoparticles remain at the oil–water interface.[51,52] The NPs in LDE-1 are located within the walls, as seen in the TEM cross section of the elastomeric wall (Figure 2a). LDE-1 undergoes interfacial initiation, and the NPs are "pushed" away from the interface and into the wall by the preferential diffusion of monomer toward the growing polymer chains at the oil–water interface. The NPs in LDE-2 form a thick layer extending from the oil–water interface to about one-third of the wall thickness, as seen in the TEM cross section of the wall (Figure 2b). The generation of this thick layer of NPs within the walls reflects the presence of two types of groups on the NP surfaces. These NPs bear both ATRP initiating groups and cross-linking groups. The NPs that function largely as initiators at the beginning of the polymerization can become "stuck" at the oil–water interface, as seen for NPs bearing ATRP initiating groups only.[51,52] However, the NPs that function largely as cross-linking centers can be driven into the wall by the preferential diffusion of monomer toward the growing chains. The competition between both driving forces yields a spectrum of behaviors and produces the thick layer of NPs in Figure 2b.

PH-2 was synthesized using a recipe identical to that of LDE-1 (Table 1) with one important difference. The recipe for PH-2 contained an organic-soluble initiator (BPO) in the external phase instead of a water-soluble initiator (KPS) in the internal phase. There were no cross-linking comonomers and no surfactants used in either of the HIPEs. PH-2 exhibits a highly interconnected, spherical structure, as seen in Figure 1f. This structure is very different from the closed-cell, polyhedral structure of LDE-1.

This difference in structure originates in the locus of initiation. Most of the polyHIPEs from Pickering HIPEs that exhibit a closed-cell-like structure are polymerized through interfacial initiation using a water-soluble initiator. In interfacial initiation, the formation of the relatively thick walls (as compared to surfactant-stabilized HIPEs) begins at the interface. Therefore, the initial stage is the formation of a solid polymer layer around the water droplet. Organic-phase initiation occurs simultaneously throughout the external phase, and a solid polymer layer around the droplet does not form in the initial stages of polymerization. The generation of closed-cell structures for interfacial initiation and open-cell structures for organic-phase initiation within identical HIPEs has been observed for other acrylate monomers.[54] PH-2 has a bimodal size distribution with averages of 85 and 400 μm, similar to, but larger than, the distribution in LDE-1. The NPs in PH-2 are located near the polymer surface, the HIPE's oil–water interface, as seen in Figure 2c. There is no preferential monomer diffusion toward the interface for organic-phase initiation, and thus the NPs are not "pushed" away from the interface, as illustrated schematically in Figure 3b,d.

Water Retention. Water retention in these materials can best be described by normalizing the water content at any time with the initial water content. The water content is the difference between $M(t)$ and $M(\infty)$. The initial water content is the difference between $M(0)$ and $M(\infty)$. The water retention behaviors of the two LDEs are similar, as seen in the log–log plot in Figure 4. The very large disparity in water retention between the LDEs and PH-2 can also be seen in Figure 4. PH-2 dries rapidly, while LDE-1 dries exceedingly slowly. The water content is reduced by 50% in 1 day for PH-2 and in 127 days for LDE-1. The drying behavior can be described using the power-law relationship in eq 1:

$$\frac{M(t) - M(\infty)}{M(0) - M(\infty)} = 1 - kt^n \quad (1)$$

where k is a constant and n is a power law exponent indicative of the release mechanism. An n of 0.50 for a slab or 0.43 for a sphere indicates that diffusion is the rate-controlling step.[59] An n of 1.0 indicates a zero-order process that is typical of evaporation. The specimens, while slablike, are actually constructed from an assembly of spheres. The n of 0.48 for LDE-1 and of 0.51 for LDE-2 indicate that diffusion is the rate-controlling step for drying in these closed-cell structures. This can be loosely compared to the diffusion of water through plant cell membranes, although the driving forces and mechanisms involved are very different. Tissues and vegetable matter usually have a water supply and slowly begin to dry when water is not available. The similarities in behaviors indicate that LDEs might be useful as model materials for tissues. The n of 0.78 for PH-2 indicates anomalous behavior, evaporation limited by the

dx.doi.org/10.1021/ma301007s | Macromolecules 2012, 45, 6450–6456

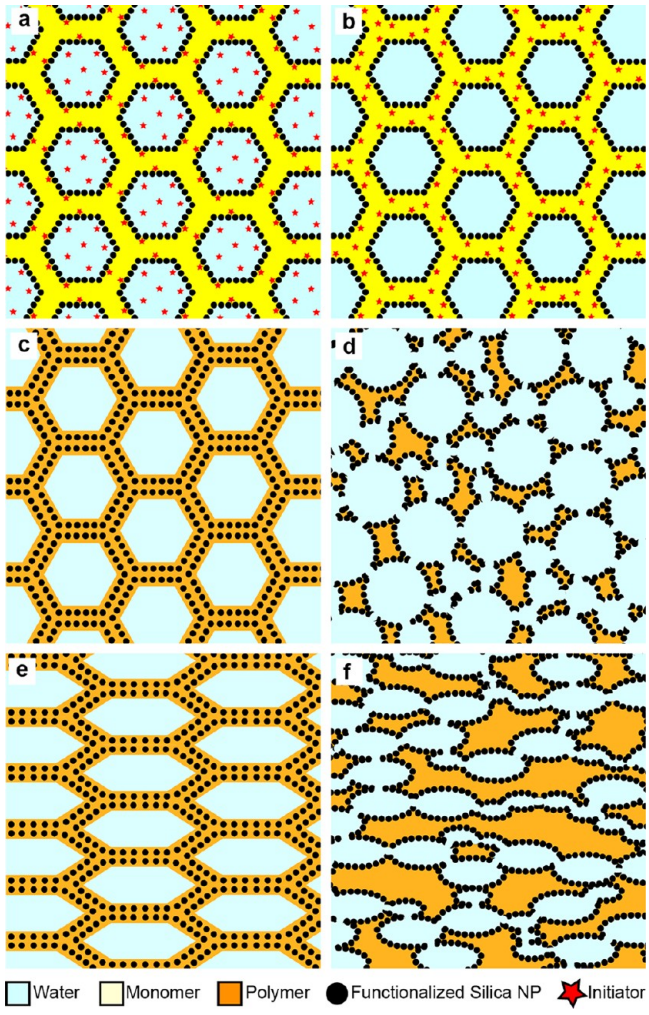

Figure 3. Schematic illustrations highlighting the differences between interfacial initiation (a, c, e) and organic-phase initiation (b, d, f): (a, b) locus of initiation; (c, d) the as-synthesized structure; (e, f) the structure under uniaxial compression with entrapped water (e) and with water expulsion (f). The wall thicknesses and the nanoparticle diameters have been highly exaggerated.

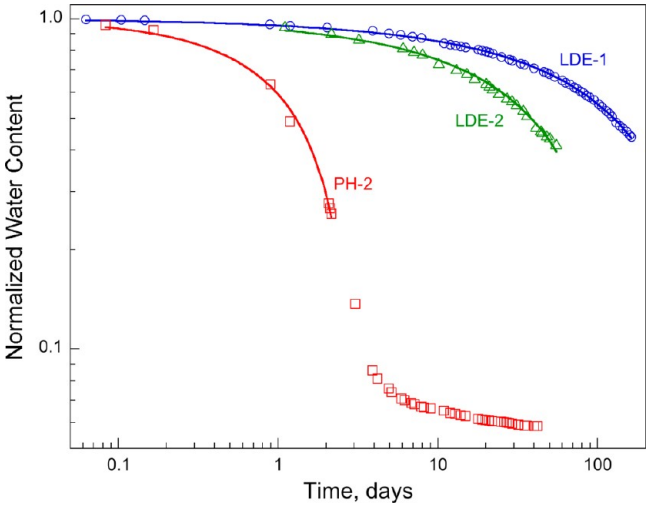

Figure 4. Log–log water retention curves for LDE-1, LDE-2, and PH-2. The solid lines are fits to the data using eq 1.

tortuous pathway through the highly interconnected polyHIPE structure.

The LDE recipe was modified in an attempt to enhance water retention. Increasing the volume fraction of the external phase from 15% to 30% increased the thickness of the elastomeric wall, which enhanced water retention. However, this enhancement in water retention was at the expense of the overall water content, which was reduced from 85% (LDE-1) to 70%. Changes in the elastomer's macromolecular structure also affected water retention. Increasing the number of cross-linking groups on the silica NPs produced thicker walls, enhancing water retention. Increasing the initiator content was also found to enhance water retention. Sealing an LDE in a water impermeable polymer film envelope significantly enhanced water retention. Sealing an undried polyHIPE within the same envelope resulted in the movement of water from the polyHIPE into the gap between the polyHIPE and the envelope.

Mechanical Behavior. PEHA is an elastomer with a glass transition temperature of −50 °C. The mechanical behavior of EHA-based surfactant-stabilized divinylbenzene-cross-linked polyHIPEs has been described previously.[36,60] The presence of entrapped water droplets significantly affects the response to an imposed deformation. The variation of compressive stress, σ_c, with compressive strain, ε_c, in uniaxial compression is seen in Figure 5. Initially (low compressive strains, high extension

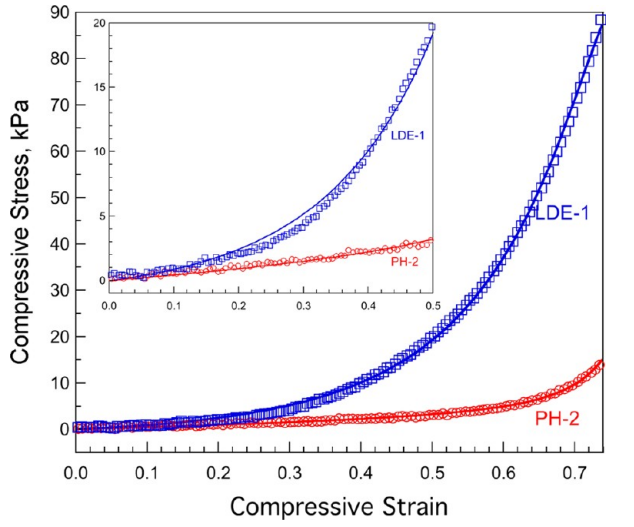

Figure 5. Mechanical behavior of LDE-1 and PH-2. The solid lines are fits to the data using eq 2.

ratios), both LDE-1 and PH-2 behave in an elastomeric manner, reflecting the elastomeric nature of the wall material. The presence of water droplets entrapped within the structure of LDE-1 has a profound influence on the mechanical behavior at larger compressive strains. During compression, water flows through the open-cell structure of PH-2, is expelled from the monolith through the external surfaces, and forms a puddle on the compression fixture. The walls of PH-2 fill the volume vacated by the water, reducing the sample volume, through a low-stress deformation mechanism, as illustrated schematically in Figure 3d,f. LDE-1 cannot deform using this mechanism since the water is entrapped within the monolith and the volume does not change, as illustrated schematically in Figure 3c,e.

dx.doi.org/10.1021/ma301007s | *Macromolecules* 2012, 45, 6450–6456

The mechanical behavior of elastomers has been described by the theory of rubber elasticity and by various phenomenological models (Mooney–Rivlin, Yeoh, and Ogden) that were derived from expansions of the strain-energy density function in terms of deformation tensor invariants.[61−64] These continuum mechanical derivations of the constitutive equations for elastomeric materials were based on the strain-energy density function, or elastic potential, which represents the change in the Helmholtz free energy of the material upon deformation. Such phenomenological models have been used successfully to describe the mechanical behavior of water-filled tissues, and they should also be appropriate for water-filled LDEs. Various phenomenological models were applied to the mechanical behavior of LDEs. Only a three-term model involving the first invariant, the second invariant, and the product of the first and second invariants was effective at describing both the relatively low stress at low compressive strains and the rapid upturn in stress at high compressive strains. The application of the model to uniaxial compression yields eq 2

$$\sigma_c = -2\left(c_{10} + \frac{c_{01}}{\lambda} + 3c_{11}\left(\lambda - \frac{1}{\lambda} + \frac{1}{\lambda^2} - 1\right)\right)\left(\lambda - \frac{1}{\lambda^2}\right) \quad (2)$$

where λ is the extension ratio (the ratio of length to initial length, $\lambda = 1 - \varepsilon_c$), and c_{10}, c_{01}, and c_{11} are the material constants associated with the first invariant, the second invariant, and a product of the two, respectively. The theory of rubber elasticity is equivalent to eq 2 with both c_{01} and c_{11} equal to zero. The Mooney–Rivlin equation is equivalent to eq 2 with c_{11} equal to zero. Cross-terms such as c_{11} have been used successfully to describe marked upswings in stress such as that seen in the LDEs.

The material constants c_{10}, c_{01}, and c_{11} from the curve fits (solid lines in Figure 5) are 1.02, −0.34, and 0.03 kPa, respectively, for PH-2. The relatively small c_{11} for PH-2 indicates that, essentially, its mechanical behavior is well described by the Mooney–Rivlin equation. The material constants are −1.37, 2.42, and −0.16 kPa, respectively, for LDE-1. The mechanical behavior of LDE-1 is more complex, and all three material constants are necessary to describe the experimental data. The compressive modulus, the limit of $d\sigma_c/d\lambda$ as λ approaches 1 (strain approaches zero), is $6(c_{10} + c_{01})$. The compressive moduli are similar, 6.3 and 4.1 kPa for LDE-1 and PH-2, respectively.

LDE-1 exhibits two behavioral regimes: there is one type of behavior at small compressive strains and another type of behavior at large compressive strains. Liquid-filled vegetable matter, which exhibits similar behavior, has been described using two different models, one for each regime of mechanical behavior.[3] At low strains the cell walls are described as bending, and their deformation is associated with a relatively low modulus. The presence of an incompressible fluid in the cell, and in all the neighboring cells, forces the cell walls to stretch when a critical strain is reached. This deformation is associated with a relatively high modulus.[3] Similarly, at low strains LDE-1 can undergo bending with low stresses. The upturn in stress is produced by stretching of the walls at high strains, as illustrated schematically in Figure 3c,e.

Flammability. The difference in flammability between a porous (air-filled) polyHIPE and a water-filled LDE can be seen in Figure 6. As soon as a flame draws close, the polyHIPE bursts into a rapidly spreading blaze and is rapidly consumed.

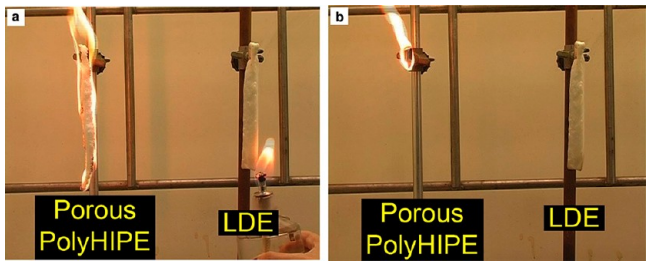

Figure 6. Photographs illustrating the differences in flammability between polyHIPEs and LDEs. The photographs are excerpts from the beginning (a) and the end (b) of the movie in the Supporting Information. The polyHIPE immediately bursts into a rapidly spreading blaze while the LDE does not undergo ignition.

This behavior can be seen in the movie in the Supporting Information. The LDE, on the other hand, does not undergo ignition, even after repeated exposures to a direct flame.

CONCLUSIONS

LDEs, elastomeric monoliths that contain around 85% water in the form of individually encapsulated micrometer-scale droplets, are an original materials concept produced using one-pot syntheses. The ability to synthesize LDEs is strongly dependent upon the type of emulsion stabilization, the type of cross-linking, and the type of initiation. The combination of NP stabilization (instead of surfactant stabilization), NP cross-linking (instead of cross-linking via comonomers), and either interfacial conventional free radical initiation or NP-based ATRP initiation (instead of organic-phase initiation) was used to successfully produce LDEs. These novel emulsion-templated materials exhibit unique properties including an extraordinary water retention, a resistance to compressive deformation similar to that seen in vegetable matter, and self-extinguishing fire retardation. The LDE materials described demonstrate a proof of concept that can be extended to other polymers and other liquids.

ASSOCIATED CONTENT

Supporting Information

A movie of the flammability test speeded up ×4. This material is available free of charge via the Internet at http://pubs.acs.org.

AUTHOR INFORMATION

Corresponding Author

*E-mail michaels@tx.technion.ac.il; Tel 972-4-829-4582.

Notes

The authors declare no competing financial interest.

ACKNOWLEDGMENTS

The partial support of the Technion VPR Fund is gratefully acknowledged.

REFERENCES

(1) Taiz, L.; Zeiger, E. *Plant Physiology*, 4th ed.; Sinauer Associates: Sunderland, MA, 2006.

(2) Alberts, B.; Johnson, A.; Lewis, J.; Raff, M.; Roberts, K.; Walter, P. *Molecular Biology of the Cell*, 4th ed.; Garland Science: New York, 2002.

(3) Warner, M.; Thiel, B. L.; Donald, A. M. *Proc. Natl. Acad. Sci. U. S. A.* **2000**, *97*, 1370–1375.

(4) Fairhurst, D.; Loxley, A. In *Science and Applications of Skin Delivery Systems*; Weichers, J., Ed.; Allured Publishing: Carol Stream, IL, 2008; Chapter 17.
(5) Lissant, K. J. *J. Colloid Interface Sci.* **1966**, *22*, 462−468.
(6) Lissant, K. J.; Peace, B. W.; Wu, S. H.; Mayhan, K. G. *J. Colloid Interface Sci.* **1974**, *47*, 416−423.
(7) Barby, D.; Haq, Z. US Pat 4,522,953, 1985.
(8) Williams, J. M.; Wrobleski, D. A. *Langmuir* **1988**, *4*, 656−662.
(9) Cameron, N. R.; Krajnc, P.; Silverstein, M. S. In *Porous Polymers*; Silverstein, M. S., Cameron, N. R., Hillmyer, M. A., Eds.; John Wiley and Sons: Hoboken, NJ, 2011; Chapter 4.
(10) Cameron, N. R.; Sherrington, D. C. *Adv. Polym. Sci.* **1996**, *126*, 163−214.
(11) Cameron, N. R.; Sherrington, D. C. *Macromolecules* **1997**, *30*, 5860−5869.
(12) Butler, R.; Davies, C. M.; Cooper, A. I. *Adv. Mater.* **2001**, *13*, 1459−1463.
(13) Butler, R.; Hopkinson, I.; Cooper, A. I. *J. Am. Chem. Soc.* **2003**, *125*, 14473−14481.
(14) Sergienko, A. Y.; Tai, H.; Narkis, M.; Silverstein, M. S. *J. Appl. Polym. Sci.* **2004**, *94*, 2233−2239.
(15) Sergienko, A. Y.; Tai, H. W.; Narkis, M.; Silverstein, M. S. *J. Appl. Polym. Sci.* **2002**, *84*, 2018−2027.
(16) Leber, N.; Fay, J. D. B.; Cameron, N. R.; Krajnc, P. *J. Polym. Sci., Part A: Polym. Chem.* **2007**, *45*, 4043−4053.
(17) Tai, H.; Sergienko, A.; Silverstein, M. S. *Polym. Eng. Sci.* **2001**, *41*, 1540−1552.
(18) Livshin, S.; Silverstein, M. S. *Macromolecules* **2008**, *41*, 3930−3938.
(19) Livshin, S.; Silverstein, M. S. *Macromolecules* **2007**, *40*, 6349−6354.
(20) Busby, W.; Cameron, N. R.; Jahoda, C. A. B. *Biomacromolecules* **2001**, *2*, 154−164.
(21) Hayman, M. W.; Smith, K. H.; Cameron, N. R.; Przyborski, S. A. *Biochem. Biophys. Methods* **2005**, *62*, 231−240.
(22) Akay, G.; Birch, M. A.; Bokhari, M. A. *Biomaterials* **2004**, *25*, 3991−4000.
(23) Stefanec, D.; Krajnc, P. *React. Funct. Polym.* **2005**, *65*, 37−45.
(24) David, D.; Silverstein, M. S. *J. Polym. Sci., Part A: Polym. Chem.* **2009**, *47*, 5806−5814.
(25) Kulygin, O.; Silverstein, M. S. *Soft Matter* **2007**, *3*, 1525−1529.
(26) Lumelsky, Y.; Zoldan, J.; Levenberg, S.; Silverstein, M. S. *Macromolecules* **2008**, *41*, 1469−1474.
(27) Lumelsky, Y.; Lalush-Michael, I.; Levenberg, S.; Silverstein, M. S. *J. Polym. Sci., Part A: Polym. Chem.* **2009**, *47*, 7043−7053.
(28) Mercier, A.; Deleuze, H.; Maillard, B.; Mondain-Monval, O. *Adv. Synth. Catal.* **2002**, *344*, 33−36.
(29) Moine, L.; Deleuze, H.; Maillard, B. *Tetrahedron Lett.* **2003**, *44*, 7813−7813.
(30) Cameron, N. R. *Polymer* **2005**, *46*, 1439−1449.
(31) Gitli, T.; Silverstein, M. S. *Soft Matter* **2008**, *4*, 2475−2485.
(32) Kovačič, S.; Jeřabek, K.; Krajnc, P. *Macromol. Chem. Phys.* **2011**, *212*, 2151−2158.
(33) Cohen, N.; Silverstein, M. S. *Macromolecules* **2012**, *45*, 1612−1621.
(34) Normatov, J.; Silverstein, M. S. *Macromolecules* **2007**, *40*, 8329−8335.
(35) Normatov, J.; Silverstein, M. S. *Polymer* **2007**, *48*, 6648−6655.
(36) Normatov, J.; Silverstein, M. S. *J. Polym. Sci., Part A: Polym. Chem.* **2008**, *46*, 2357−2366.
(37) Normatov, J.; Silverstein, M. S. *Chem. Mater.* **2008**, *20*, 1571−1577.
(38) Menner, A.; Powell, R.; Bismarck, A. *Soft Matter* **2006**, *4*, 337−342.
(39) Haibach, K.; Menner, A.; Powell, R.; Bismarck, A. *Polymer* **2006**, *47*, 4513−4519.
(40) Menner, A.; Haibach, K.; Powell, R.; Bismarck, A. *Polymer* **2006**, *47*, 7628−7635.
(41) Tai, H.; Sergienko, A.; Silverstein, M. S. *Polymer* **2001**, *42*, 4473−4482.
(42) Silverstein, M. S.; Tai, H.; Sergienko, A.; Lumelsky, Y.; Pavlovsky, S. *Polymer* **2005**, *46*, 6682−6694.
(43) Desforges, A.; Backov, R.; Deleuze, H.; Mondain-Monval, O. *Adv. Funct. Mater.* **2005**, *15*, 1689−1695.
(44) Pickering, S. U. *J. Chem. Soc.* **1907**, *91*, 2001−2021.
(45) Menner, A.; Verdejo, R.; Shaffer, M.; Bismarck, A. *Langmuir* **2007**, *23*, 2398−2403.
(46) Menner, A.; Ikem, V.; Salgueiro, M.; Shaffer, M. S. P.; Bismarck, , A. *Chem. Commun.* **2007**, 4274−4276.
(47) Colver, P. J.; Bon, S. A. F. *Chem. Mater.* **2007**, *19*, 1537−1539.
(48) Ikem, V. O.; Menner, A.; Bismarck, A. *Angew. Chem., Int. Ed.* **2008**, *47*, 8277−8279.
(49) Ikem, V. O.; Menner, A.; Horozov, T. S.; Bismarck, A. *Adv. Mater.* **2010**, *22*, 3588−3592.
(50) Zhang, S.; Chen, J. *Chem. Commun.* **2009**, 2217−2219.
(51) Gurevitch, I.; Silverstein, M. S. *Macromolecules* **2011**, *44*, 3398−3409.
(52) Gurevitch, I.; Silverstein, M. S. *J. Polym. Sci., Part A: Polym. Chem.* **2010**, *48*, 1516−1525.
(53) Chen, Y.; Ballard, N.; Gayet, F.; Bon, S. A. F. *Chem. Commun.* **2012**, *48*, 1117−1119.
(54) Gurevitch, I.; Silverstein, M. S. *Soft Matter* DOI: 10.1039/C2SM26404H.
(55) Min, K.; Gao, H.; Matyjaszewski, K. *J. Am. Chem. Soc.* **2005**, *127*, 3825−3830.
(56) Min, K.; Matyjaszewski, K. *Macromolecules* **2005**, *38*, 8131−8134.
(57) Min, K.; Gao, H.; Matyjaszewski, K. *J. Am. Chem. Soc.* **2006**, *128*, 10521−10526.
(58) Carnachan, R. J.; Bokhari, M.; Przyborski, S. A.; Cameron, N. R. *Soft Matter* **2006**, *2*, 608−616.
(59) Ritger, P. L.; Peppas, N. A. *J. Controlled Release* **1987**, *5*, 23−36.
(60) Andrews, R. A.; Grulke, E. A. In *Polymer Handbook*, 4th ed.; Brandrup, J., Immergut, E. H., Grulke, E. A., Eds.; John Wiley and Sons: NewYork, 1999; Chapter VI.
(61) Tschoegl, N. W. *J. Polym. Sci., Part A-1: Polym. Chem.* **1971**, *9*, 1959−1970.
(62) Laraba-Abbes, F.; Ienny, P.; Piques, R. *Polymer* **2003**, *44*, 821−840.
(63) Ogden, R. W. *Proc. R. Soc. London, A* **1972**, *326*, 565−584.
(64) Yeoh, O. H. *Rubber Chem. Technol.* **1993**, *66*, 754−771.